Fermi-Edge Singularities in $Al_xGa_{1-x}As$ Quantum Wells: Extrinsic versus Many-Body Scattering Processes

T. Mélin* and F. Laruelle

Laboratoire de Microstructures et de Microélectronique, Centre National de la Recherche Scientifique, 196 Avenue Henri Ravera, BP 107, 92225 Bagneux Cedex, France
(Received 10 February 2000)

A Fano resonance mechanism is evidenced to control the formation of optical Fermi-edge singularities in multisubband systems such as remotely doped $Al_xGa_{1-x}As$ heterostructures. Using Fano parameters, we probe the *physical nature* of the interaction between Fermi sea electrons and empty conduction subbands. We show that processes of extrinsic origin like alloy disorder prevail easily at 2D over multiple diffusions from charged valence holes expected by many-body scenarios.

PACS numbers: 78.66.–w, 71.10.Ca, 71.35.–y, 73.20.Dx

Drastic manifestations are expected from the interaction of a magnetic or charged impurity with a Fermi sea of electrons [1]. Since the successful explanation of the divergent x-ray absorption edges of simple metals [2] by Mahan [3] and Nozières *et al.* [4] some thirty years ago, a Fermi sea of electrons under optical excitation has been recognized as a model system to study these issues experimentally. Indeed a many-body electronic state can develop in the presence of the positively charged electronic vacancy (or core hole) involved in optical processes, which multiply scatters conduction electrons throughout and along the Fermi surface. This induces divergences at the Fermi edge of optical spectra, the so-called Fermi-edge singularities (FES). FES are by essence highly sensitive to phase space restrictions such as hole localization and reduced dimensionalities: they cannot form without either strong hole localization or the dimensionality being unity [5].

Electron systems embedded in semiconductor heterostructures have therefore attracted much attention to test these predictions [6]. FES were first observed by Skolnick *et al.* [7] in the low-temperature photoluminescence (PL) spectrum of a remotely doped $In_{0.47}Ga_{0.53}As/InP$ quantum well (QW). Emphasis was put on the anomalous temperature dependence of the singularity and on the localization of valence holes by alloy fluctuations. More recently, experiments by Chen *et al.* [8] in $In_{0.15}Ga_{0.85}As/AlGaAs$ QWs with weaker hole localization also put forward the *tunability* of FES, by bringing the first empty QW subband into resonance with the Fermi level. It was then proposed that empty conduction subbands could act as additional scattering channels for Coulomb processes, in qualitative agreement with many-body multisubband numerical calculations in the infinite hole-mass approximation [9].

Although this interpretation is widely referred to, no experiments have been undertaken to test many-body schemes beyond qualitative agreement. While attempting to do so with $Al_xGa_{1-x}As$ QWs, it appeared to us that *non-Coulombian* intersubband scatterings can induce FES as well. The scope of this Letter is to describe this issue quantitatively. Our experiments demonstrate that extrinsic processes like alloy disorder can prevail easily over multiple Coulomb scatterings of Fermi sea electrons predicted in the framework of many-body scenarios.

The paper is organized as follows. We show that the formation of FES in $Al_xGa_{1-x}As$ QWs is governed by a Fano resonance mechanism [10] between Fermi-sea electrons and discrete excitonic transitions associated with empty conduction subbands. This model is first validated by the existence of scaling properties of PL spectra when FES are enhanced by reduced intersubband spacings. It is then used to gain insight into the microscopic nature of conduction intersubband couplings (ICs) at work. Indeed, the stronger the ICs, the more divergent the FES, so that one can probe directly in experiments the efficiency of extrinsic scattering processes such as alloy disorder, remote-doping disorder, or artificial ICs in lateral superlattices [11]. Experimental results fall in close agreement with microscopic Fano calculations. We demonstrate that alloy disorder is the dominant contribution to observed FES in $Al_xGa_{1-x}As$ QWs.

Samples investigated in this work are remotely doped $Al_xGa_{1-x}As/Al_{0.33}Ga_{0.67}As$ QWs grown on GaAs substrates by molecular beam epitaxy. They are all of the same thickness $L_z = 25$ nm, spacers (in the range 5–8 nm) and sheet density $n_s \simeq 8.10^{11}$ cm^{-2}, but vary in their aluminum content x ($2.3\% \leq x \leq 7.1\%$). Confined 2D levels are represented in Fig. 1a. The asymmetry of the QW potential originates in the dipole formed by remote ionized dopants ($z > 0$) and the degenerate electron gas (DEG) partially filling the first conduction subband E_1. This confers a PL activity to the two first subbands E_1 and E_2 with photocreated valence holes localized on potential fluctuations at the top of the heavy-hole HH_1 subband (Fig. 1b). We perform PL spectroscopy at 1.8 K. Samples are optically excited by a Ti:Sa laser at 1.7 eV, with a $\simeq 1$ W cm^{-2} density so as to avoid inhomogeneous heating of the DEG within the 40 μm diameter laser spot. The DEG PL (E_1HH_1) extends from lowest wave-vector transitions at E_g up to Fermi wave-vector transitions at $E_g + E_F$ ($E_F \simeq 25$ meV). Without any influence of E_2HH_1, its oscillator strength decreases monotonously with energy,

                   © 2000 The American Physical Society
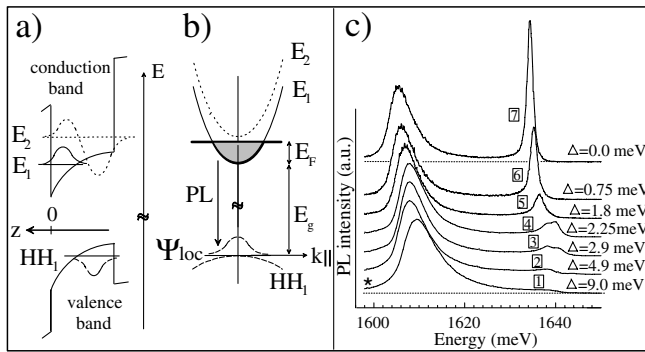
FIG. 1. (a) Schematic 2D-confined conduction and valence envelope functions for E_1, E_2, and HH_1. Remote δ doping is achieved on the $z > 0$ side. (b) In-plane k-space band structure showing the PL recombination of Fermi-sea electrons with photocreated holes at $T = 0$ K. Localized HH_1 states are sketched by a k-space extended wave function Ψ_{loc}. (c) 1.8 K PL spectra of sample A recorded for various Δ values.

because of hole localization and indirect optical processes [12] (see spectrum $\star$ in Fig. 1c). The PL of the empty QW subband E_2 exhibits a dominant excitonic feature E_{2_x} of high oscillator strength and discrete character, visible either by thermal activation above $E_g + E_F$ in PL, or in PL excitation spectra. We define $\Delta = E_{2_x} - E_g - E_F$. Variations of Δ are achieved along a given sample by use of the flux gradients of effusion cells in the epitaxy chamber. We stop the wafer rotation during the spacer layer growth between dopants and the QW. The thinner the spacer, the stronger the electric field at the QW interface. This tunes the $E_2 - E_1$ energy separation, while E_F hardly changes under illumination [13]. As seen from PL spectra of sample A ($x = 7.1\%$) in Fig. 1c, a FES forms and develops [8] when Δ is decreased to zero [14].

To interpret these data, we consider the Fano resonance model depicted in Fig. 2a. E_{2_x} is taken as a discrete level coupled with a matrix element $\mathcal{W}$ to the continuum of E_1HH_1 electron-hole pairs. By assuming an infinite hole mass, all physical parameters simply refer to the conduction band: $\mathcal{W}$ equals to the IC between E_1 and E_2, and the E_1HH_1 continuum is populated by the E_1 Fermi-Dirac electrons. We take a parabolic dispersion and a constant PL oscillator strength for E_1. Fano [10] gave an analytical description of the spreading of a discrete level coupled to a continuum. Optical FES occur (see Fig. 2a) due to the partial filling of E_1HH_1 near E_{2_x} and get more divergent as Δ is reduced. A qualitative agreement with experiments [8] is thus obtained, without any particular assumption on the physical nature of $\mathcal{W}$.

The validation of the Fano resonance model comes from the scaling property evidenced in Fig. 2a that all PL spectra for various Δ should display a common envelope line shape when plotted with E_{2_x} as the origin of energies. The comparison with experimental data is not straightforward because $E_1 - E_2$ varies experimentally, while the E_1HH_1 PL oscillator strength intrinsically depends on energy [12].
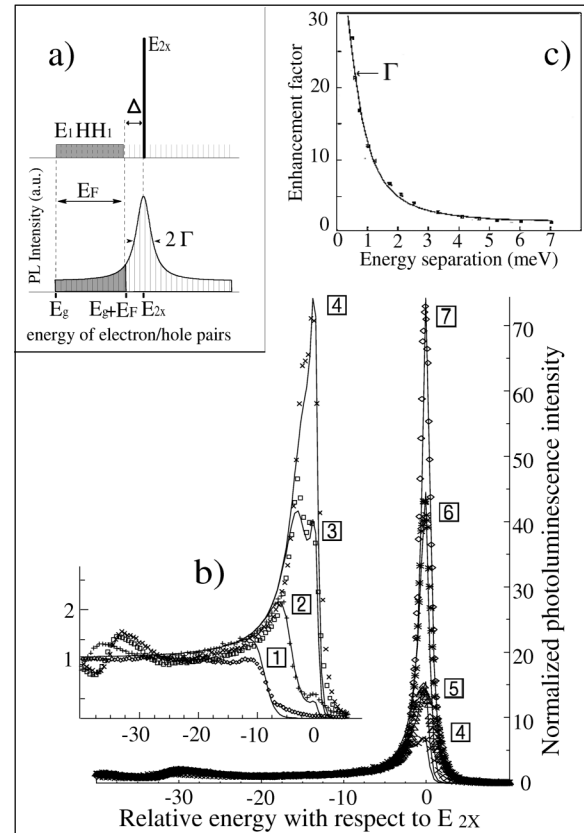
FIG. 2. (a) Fano resonance model, where E_{2_x} is seen as a discrete level in the E_1HH_1 continuum (top). In the coupled system (bottom), a FES appears, due to the partial filling of E_1 (dark grey). 2Γ is the resonance width. (b) Points: data of Fig. 1c, normalized by the PL spectrum with $\Delta \rightarrow \infty$ ($\star$ in Fig. 1c) and plotted with E_{2_x} as the origin of energies. Lines: fits using a Fano profile ($q = 12.2$ and $\Gamma = 0.60$ meV) and Fermi-Dirac electrons ($T = 9.0 \pm 1$ K). (c) FES "enhancement factor" (points, from Ref. [8]) in an $In_{0.15}Ga_{0.85}As$ QW, fitted (line) by a Fano profile with $\Gamma = 0.66$ meV and $q = 6.6$.

We compensate for these nominal E_1HH_1 PL variations by dividing all data of Fig. 1c by the E_1HH_1 spectrum with $\Delta \rightarrow \infty$ ($\star$ in Fig. 1c). Data are then plotted in Fig. 2b with E_{2_x} as the origin of energies. Remarkably, all spectra superpose on each other in the range of populated electron states [15]. No clear transition exists from convergent to divergent Fermi edges in Fig. 2b. This means that FES appear only in raw PL data when the intrinsic PL decay of E_1HH_1 at E_F gets balanced by the positive slope of the Fano envelope for small Δ values.

In order to get a quantitative analysis of the envelope profile, we assume a statistical disorder property for the interaction $\mathcal{W}$: $\langle \mathcal{W} \rangle = 0$ and $\langle \mathcal{W}^2 \rangle \neq 0$. This accounts for alloy disorder, which is later evidenced to dominate FES in sample A. The *normalized* PL intensity can then be derived analytically from Ref. [10]:

$$I(E) = f(E) \frac{q^2 + (E - E_{2_x})^2/\Gamma^2}{1 + (E - E_{2_x})^2/\Gamma^2},$$

where E is the PL energy, $f(E)$ is the occupation number in the E_1 subband, Γ is the observed half width at half maximum of the resonance, only related to the statistical squared interaction average $\langle \mathcal{W}^2 \rangle$ and the density of states $\mathcal{D}$ of the E_1 conduction subband by $\Gamma = \pi \langle \mathcal{W}^2 \rangle \mathcal{D}$, and q^2 is the experimental oscillator strength of the excitonic resonance relative to the continuum, inversely proportional to $\langle \mathcal{W}^2 \rangle$ and $\mathcal{D}^2$. It depends also strongly on wave function overlaps through the ratio of the oscillator strengths of $E_2 HH_1$ and $E_1 HH_1$. q^2 is therefore quite sensitive to small geometrical fluctuations from sample to sample.

Our data are nicely fitted by this model (Fig. 2b), with Fano parameters $\Gamma = 0.60$ meV and $q = 12.2$. All fits use Fermi-Dirac distributions of electrons with an effective temperature $T = 9.0 \pm 1$ K. This shows that electrons are indeed thermalized, though not with the lattice at 1.8 K due to the incomplete and slow relaxation of photo-created electrons above the E_2 subband edge. The consistence of small Δ data with our fit indicates that the E_{2x} resonance remains weakly populated enough to stay in the "atomlike" regime [16]. Also, taking $f(E) = 1$ in the Fano line shape formula, we can check that it fits the FES enhancement factor (FES PL intensity divided by its $\Delta \rightarrow \infty$ value) measured by Chen *et al.* in $In_{0.15}Ga_{0.85}As$ QW structures [8]. Their data are indeed nicely reproduced with $\Gamma = 0.66$ meV and $q = 6.6$ (Fig. 2c).

Before quitting the phenomenological level, we focus on the temperature dependence of FES in systems with explicit intersubband interaction. Observed thermal quenchings can be understood simply, even though such quenchings are expected from many-body theories [17], where an actual occupation number discontinuity is required to enhance multiple Coulomb scatterings at E_F. Here or in Ref. [8], the FES disappears, only because the PL relative minimum between $E_g + E_F$ and E_{2x} vanishes with raised temperatures [18].

Up to this point, we successfully assessed the model with respect to Δ and temperature variations. We now analyze the microscopic origin of the Fano parameter Γ. On the theoretical side, Γ only depends on the strength $\mathcal{W}$ of intersubband couplings and can be computed for a given microscopic process. Experimentally, the Fano model predicts that the stronger the Γ parameter the more divergent the Fermi edges at fixed Δ. By designing appropriate samples, one can thus test (i) whether extrinsic scattering processes like alloy disorder play an effective role on the formation of FES or (ii) if experimental variations of Γ correlate with microscopic calculations.

We display in Fig. 3a the PL spectra of remotely doped quantum wells C, B, and A of QW aluminum content x equal to 0.023, 0.044, and 0.071, respectively, taken at fixed $\Delta = 4.3 \pm 0.1$ meV. As seen from the global PL line shapes, the localization of photocreated valence holes remains constant, dominated by the roughness at the QW interface (see Fig. 1) rather than by random alloy potential fluctuations. Enhancement of many-body
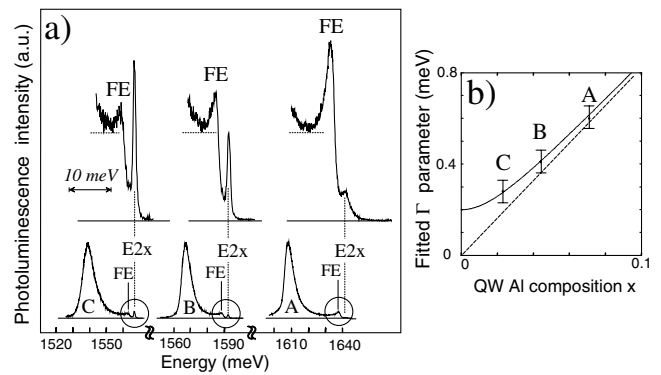
FIG. 3. (a) 1.8 K PL of samples C, B, and A taken at $\Delta = 4.3 \pm 0.1$ meV. The Fermi-edge regions are zoomed in. (b) Fitted Fano parameters Γ as a function of alloy content. Microscopic calculations are given without (dotted line) and with (full line) a residual disorder $\Gamma_0 = 0.2$ meV (see text).

processes due to hole localization [5,7] can therefore be excluded. Nevertheless, FES get more pronounced with increased alloy concentration x, while the excitonic resonance broadens. Fitted Γ Fano parameters [19] linearly increase with x within experimental uncertainty (Fig. 3b). This explains the quadratic enhancement of FES visible from Fig. 3a when Γ is linearly increased in the regime where $\Delta / \Gamma \gg 1$. It also demonstrates that alloy disorder is the dominant contribution to the IC parameter $\mathcal{W}$.

To quantify this, we calculate Γ microscopically in the infinite hole-mass approximation [20]:

$$\Gamma_{\text{alloy}} = x(1 - x)m^\star \Omega_0 \delta V^2 / L_z \hbar^2.$$

This applies for a square quantum well of width L_z, a conduction effective electron mass $m^\star$, δV being the conduction band offset between pure AlAs and pure GaAs, and Ω_0 being the crystal cell volume. With $L_z = 18$ nm (representative of the confinement length of E_1 and E_2 wave functions), $m^\star = 0.07 m_0$ and $x = 7.1\%$, we obtain $\Gamma = 0.61$ meV. This quantitative agreement is striking for such a simple model. The fit from Fig. 3b is achieved by introducing a residual scattering $\Gamma_0 = 0.2$ meV in the pure GaAs limit and thus taking a Fano parameter $\Gamma^2 = \Gamma_0^2 + \Gamma_{\text{alloy}}^2$. We can also estimate $\Gamma_{\text{alloy}} \simeq 0.5$ meV for the $In_{0.15}Ga_{0.85}As$ QWs of Ref. [8], in close agreement with either our fit (Fig. 2c) or the empirical two-level coupling (0.6 meV) measured by Chen *et al.*

We now focus on ICs induced by random positioning of ionized dopants. Strictly speaking, $\mathcal{W}$ now depends on the occupation of E_1 states. We nonetheless assume $\mathcal{W}$ equal to its value for Fermi wave-vector (k_F) electrons. Γ can then be computed [21] and gets proportional to $\exp{-2k_F z_0}$ in the limit of a thick spacer layer z_0, with a prefactor of $\simeq 60$ meV for a square QW structure of width $L_z = 20$ nm and a sheet density $n_s \approx 10^{12}$ cm^{-2}. Because of high doping ($k_F \gtrsim 2.10^8$ m^{-1}), this predicts a poor efficiency even for very shallow spacers. This is already visible from Fig. 2b where indirect optical processes

[12]—of the same physical origin—only affect small wave-vector conduction states. Also, we measured no increase of Γ in a sample similar to C but with a 2.5 nm spacer.

We finally mention the case of FES in tilted lateral superlattices, where artificial intersubband couplings are created by a nonseparable 1D periodic confinement between the growth (z) and an in-plane (x) direction. This has been shown to promote optical FES [11]. In fact, our data also fit to a Fano scheme [21] with parameter $\Gamma = 3.2$ meV. The larger strength of ICs compared to 2D QWs explains the formation of pronounced FES even for large Δ parameters [11]. The experimental Γ value matches a microscopic calculation, using a typical value of 30 meV for the peak-to-peak lateral confinement amplitude [22].

Microscopic calculations of Fano parameters fall therefore in quantitative agreement with our experiments, where ICs have been varied in physical nature and over one decade in amplitude. This demonstrates that non-Coulombian scattering processes can efficiently control the formation of FES in multisubband semiconductor structures, in the simple picture of a band structure partially filled by a DEG. We stress that Coulomb processes actually depend on the accurate distribution of charged particles with respect to empty subbands and *do not* quantitatively match Fano line shapes [9], even if a qualitative analogy was underlined in early many-body interpretations [8,9]. The question of extrinsic ICs can also be raised about Ref. [7]. A FES enhancement of a factor $\simeq 2$ would correspond to $q \simeq \Delta/\Gamma$ for a Fano process involving empty subbands. Estimating $\Delta \simeq 30$ meV [7] and $\Gamma_{\text{alloy}} = 1.0$ meV, this criterium discards random alloy-disorder processes provided $q \ll 30$. An evaluation of actual disorder processes and relevant absorption data on E_{2_x} are definitely lacking to give any conclusive answer, but the QW doping on both sides used in Ref. [7] should reduce advantageously the E_2 and HH$_1$ overlap and thus q. Bringing q values down by optical selection rules indeed suppresses excitonic enhancement effects [9].

In conclusion, this paper shows that extrinsic intersubband scatterings must be carefully evaluated while analyzing FES. This applies especially to lower dimensionality issues [5] since disorder gets generally enhanced, and conduction subband spacings lowered. Realistic many-body theories should thus include disorder and multiple subbands. Our work should extend under magnetic field where the interaction of excitons and a DEG is debated [23]. Extremely low-disorder structures seem required for clear electron-electron manifestations [24].

*Permanent address: Institut d'Electronique et de Microélectronique du Nord (IEMN)–Department ISEN, BP 69, Avenue Poincaré, 59652 Villeneuve d'Ascq, France. Email address: thierry.melin@isen.iemn.univ-lille1.fr

[1] See, e.g., G. D. Mahan, *Many Particle Physics* (Plenum, New York, 1990).

[2] For a review, see P. H. Citrin, G. K. Wertheim, and M. Schlüter, Phys. Rev. B **20**, 3067 (1979).

[3] G. D. Mahan, Phys. Rev. **153**, 882 (1967).

[4] P. Nozières and C. T. De Dominicis, Phys. Rev. **178**, 1097 (1969).

[5] See, e.g., P. Nozières, J. Phys. I **4**, 1275–1280 (1994).

[6] See, e.g., G. E. W. Bauer, Phys. Rev. B **45**, 9153 (1992), and references therein.

[7] M. S. Skolnick, J. M. Rorison, K. J. Nash, D. J. Mowbray, P. R. Tapster, S. J. Bass, and A. D. Pitt, Phys. Rev. Lett. **58**, 2130 (1987).

[8] W. Chen, M. Fritze, W. Walecki, A. V. Nurmikko, D. Ackley, J. M. Hong, and L. L. Chang, Phys. Rev. B **45**, 8464 (1992).

[9] J. F. Mueller, Phys. Rev. B **42**, 11 189 (1990); P. Hawrylak, Phys. Rev. B **44**, 6262 (1991).

[10] U. Fano, Phys. Rev. **124**, 1866 (1961).

[11] T. Mélin and F. Laruelle, Phys. Rev. Lett. **76**, 4219 (1996).

[12] S. K. Lyo, E. D. Jones, and J. F. Klem, Phys. Rev. Lett. **61**, 2265 (1988).

[13] This enables experiments similar to Ref. [8], where Chen *et al.* used an in-plane magnetic field to tune Δ.

[14] Reported Δ values stem from the fit in Fig. 2b (see text). They fall in close agreement with magneto-optical PL data, which provide an actual measurement of $E_g + E_F$.

[15] Small discrepancies occur around the low-energy peak of the DEG PL, all the more pronounced with thinner spacer layers. This shows the increased efficiency of indirect optical processes for less remote dopants, while they are taken constant in the normalization procedure.

[16] A strong population of E_{2_x} would alter its atomlike excitonic character, both in PL and PL excitation spectra: T. A. Fisher, P. E. Simmonds, M. S. Skolnick, A. D. Martin, and R. S. Smith, Phys. Rev. B **48**, 14 253 (1993).

[17] See, e.g., K. Ohtaka and Y. Tanabe, Phys. Rev. B **39**, 3054 (1989), and references therein.

[18] The same happens when Δ is reduced at fixed temperature (see, e.g., $\Delta = 2.9$ and 2.25 meV in Figs. 1c and 2b).

[19] In Fig. 3b, Γ is *fitted* from $\Delta \rightarrow 0$ PL data, rather than measured directly from the E_{2_x} resonance width in large Δ spectra. This is more relevant, since, for instance, the high-energy side of E_{2_x} is affected by the luminescence of the E_2HH$_1$ continuum (visible in Fig. 2b where fits systematically underestimate the PL signal above E_{2_x}).

[20] See, e.g., G. Bastard, *Wave-Mechanics Applied to Semiconductor Structures* (Les Editions de Physique, Les Ulis, France, 1988).

[21] T. Mélin and F. Laruelle (to be published).

[22] T. Mélin and F. Laruelle, Phys. Rev. Lett. **81**, 4460 (1998).

[23] W. Chen *et al.,* Phys. Rev. Lett. **64**, 2434 (1990); M. S. Skolnick *et al.,* Phys. Rev. Lett. **66**, 963 (1991); W. Chen *et al.,* Phys. Rev. Lett. **66**, 964 (1991).

[24] L. Gravier, M. Potemski, P. Hawrylak, and B. Etienne, Phys. Rev. Lett. **80**, 3344 (1998).